OPEN ACCESS
IOP Publishing
Journal of Physics D: Applied Physics
J. Phys. D: Appl. Phys. **56** (2023) 045001 (11pp)
https://doi.org/10.1088/1361-6463/aca988

Electromechanical behaviour of REBCO coated conductor toroidal field coils for ultra-high-field magnetic-confinement plasma devices

Xiaodong Li[1,*], Veit Große[2], Dongbin Song[3], Wenjiang Yang[3] and Rafael Macián-Juan[1]

[1] Chair of Nuclear Technology, School of Engineering and Design, Technische Universität München (TUM), 85748 Garching b. München, Germany
[2] Department of Research and Development, Theva Dünnschichttechnik GmbH, Gewerbegebiet Am Lenzenfleck, Rote-Kreuz-Straße 8, 85737 Ismaning, Germany
[3] School of Astronautics, Beihang University (BUAA), 100191 Beijing, People's Republic of China

E-mail: xiaodong.li@tum.de

Received 29 April 2022, revised 3 December 2022
Accepted for publication 7 December 2022
Published 15 December 2022

Abstract

The development of rare-earth barium copper oxide (REBCO) coated conductors with an extremely high critical current density under ultra-high fields opens up a high-field path towards large-scale fusion. The latest technology has inspired cable-in-conduit conductors such as conductor on round core wires, twisted stacked tape conductor cables and Rutherford cables with outstanding current-carrying capacities. In order to realise an inductance balance and decrease magnetic diffusion, these cables have been twisted or folded to a certain extent, thus breaking the mechanical behaviour of the ceramic superconductor and limiting their potential for ultra-high-field applications. One possible solution is to employ a non-twisted cable, which offers maximum protection of its mechanical properties and enables a parallel orientation of the toroidal field vector to the surface of REBCO coated conductors, and at the same time decreases the influence of perpendicular fields on the critical current of REBCO cables. However, the applied physics community's attitude towards using non-twisted, parallel REBCO stacked-tape cables is one of scepticism, the main argument being that the nonlinear **E**–**J** behaviour associated with screening current in the parallel stack might lead to a field distortion and reduce the performance of superconductivity. Recent analyses have demonstrated that the effect of screening current decreases significantly owing to a wavelike magnetic field distribution along the cable. The authors obtained similar results using **H**-formulation and **T**–**A** formulation based finite element methods and demonstrated that the non-twisted cable may be feasible for DC current transmission toroidal field coils in magnetic-confinement devices. Furthermore, the electromechanical behaviour of toroidal field coils has been evaluated via the Maxwell stress, solved by using an **A**–**V** formulation. It was discovered that the stress generated by the toroidal

* Author to whom any correspondence should be addressed.

Original content from this work may be used under the terms of the Creative Commons Attribution 4.0 licence. Any further distribution of this work must maintain attribution to the author(s) and the title of the work, journal citation and DOI.

 © 2022 The Author(s). Published by IOP Publishing Ltd

field coils is within the stress tolerance of the REBCO coated conductor, something which is of great significance in promoting the application of REBCO coated conductors for ultra-high-field magnetic-confinement plasma devices.

Keywords: ultra-high-field, REBCO coated conductor, magnetic-confinement plasma, toroidal field coils

(Some figures may appear in colour only in the online journal)

1. Introduction

The global race for fusion energy on earth is mainly a story of magnetic-confinement plasma [1]. Ultra-high magnetic fields can decrease particle drifting and disruption, and significantly increase the possibility of fusion reactions. The international thermonuclear experimental reactor (ITER) has a fusion energy gain factor of 10 and aims to achieve a peak magnetic flux density of 11.8 Tesla by using low temperature superconducting (LTS) Nb_3Sn conductors [2]. However, things may change with the emergence of the second-generation high temperature superconducting (HTS) rare-earth barium copper oxide (REBCO) coated conductor, a technique that was not introduced when the ITER project was launched but which has reached a certain degree of maturity so that there are now tens of manufacturers worldwide [3]. Over the last 15 years, REBCO coated conductors have made great strides toward potential applications in motors [4], fault current limiters [5], magnetic energy storage systems [6], transformers [7], wind turbine generators [8], magnetic resonance imaging (MRI) machines and so on [9]. They are regarded as a breakthrough for the new generation of ultra-high-field (>20 Tesla) fusion power plants [10]. The current baseline design for the toroidal field coils and central solenoid coils of the European Demonstration Power Plant (EU-DEMO) reactor is based on Nb_3Sn conductors. High temperature superconductor activities have been pursued in parallel to the LTS coils, the mid-term target has been focused on determining the best REBCO cable option for fusion magnets [11]. The CFETR-Phase II fusion project aims to enhance the magnet system by using REBCO magnets [12, 13]. In addition, REBCO coated conductor cables with current capacity of 100 kA are being built and tested for the magnet system of the force-free helical reactor in Japan [14–16]. A helical current-carrying element made of REBCO coated conductors is also under development for the fusion neutron source in Russia [17]. Since a compact fusion reactor project relying entirely on REBCO magnets was launched in the United States in 2020 [18], the design of REBCO cables for large-scale fusion reactors has got into full swing. At present, existing REBCO cabling methods for fusion are mainly based on the cable-in-conduit conductor (CICC) technique, which has derived many cable designs such as twisted stacked tape conductor (TSTC) cables [19, 20], conductor on round core (CORC) cables [21], Rutherford cables [22] and star conductors [23]. In our previous study, the current-carrying capacity and magnetic behaviour of TSTC cables were estimated by finite element methods; it was discovered that the REBCO cable has a high-current-carrying capacity in a low-temperature cooling environment [24]. However, it might be quite challenging to employ the cable as a component for toroidal field coils in a compact fusion reactor because mechanical issues caused by bending after twisting might lead to an enormous critical current degradation. In addition, experiments show that the bending strain and the twist pitch have a negative impact on current-carrying capacity of TSTC cables [25, 26]. The degradation of I_c in CORC cables caused by mechanical pinching has also been detected [27]. An I_c reduction was observed during the cyclic transverse load in experimental tests [22]. The non-twisted, star cable seems to have a predictable and stable electromechanical performance [23]. Nevertheless, the high copper ratio in the cable might lead to high eddy-current losses under current ramping conditions.

The advantage of the non-twisted cable design is its high tolerance to transverse stress [28] and extremely high critical current density, since there is no critical current decay caused by torsion. A recently analysis proposed the possibility of using non-twisted paralleled REBCO stacked-tape as the cable for toroidal field coils [29], and it has been demonstrated that a wavelike magnetic field distribution along the conductor can significantly decrease the negative effect of the screening currents induced during charging. In this article, a similar wavelike magnetic field was obtained by using **T**–**A** formulation and **H**-formulation based finite element methods. In addition, the electromechanical behaviour of toroidal field coils consisting of non-twisted CICC cables has been studied further using an **A**–**V** formulation. The results demonstrate the feasibility of employing non-twisted CICC cables for ultra-high-field magnetic-confinement plasma devices.

2. Numerical scheme

The studies were carried out by using **H**-formulation [30–32], **T**–**A** formulation [33, 34] and **A**–**V** formulation [35, 36] based finite element methods. **H**-formulation and **T**–**A** formulation are employed to study power loss, eddy-current loss and magnetic behaviour of the non-twisted cable, while **A**–**V** formulation is mainly used for the analysis of magnetic and mechanical behaviour of the large-scale toroidal field module coils. Descriptions of these methods are shown as follows.

The **E**–**J** power law of the REBCO coated conductor has been observed experimentally and can be described as:

$$\mathbf{E} = E_0 \left| \frac{J}{J_c(B_{\parallel}, B_{\perp}, T)} \right|^n \frac{\mathbf{J}}{|J|}. \tag{1}$$

This model can be used in superconductivity theories on magnetic flux penetration, AC loss susceptibility, flux creep and critical state analysis [37]. It can be concluded from equation (1) that the nonlinear resistivity of the REBCO conductor is:

$$\rho = \frac{E_0}{J_c(B_\parallel, B_\perp, T)} \cdot \left| \frac{J}{J_c(B_\parallel, B_\perp, T)} \right|^{n-1}. \tag{2}$$

The Kim model is normally used to describe the dependence of the critical current density J_c on the magnetic field [38], and here the model is further optimised by considering the temperature dependence of J_c and can be described as:

$$J_c(B_\parallel, B_\perp, T) = \frac{J_{c0}}{\left[1 + \sqrt{(kB_\parallel)^2 + {B_\perp}^2}/B_0\right]^\alpha} \cdot \left[1 - \left(\frac{T}{T_c}\right)^2\right]^{3/2}. \tag{3}$$

In the **H**-formulation, **H** stands for the magnetic field strength. The current density **J** in the solution domain can be derived via the quasi-static approximation of the Maxwell–Ampere's law as:

$$\nabla \times \mathbf{H} = \mathbf{J}. \tag{4}$$

The electromagnetic behaviour of the REBCO conductor domain should satisfy the Maxwell–Faraday's law as:

$$\nabla \times \mathbf{E} = -\frac{\partial \mathbf{B}}{\partial t}. \tag{5}$$

Therefore, it can be rewritten by considering the dependent variable **H** as:

$$\frac{\partial(\mu_0 \mu_r \mathbf{H})}{\partial t} + \nabla \times (\rho \nabla \times \mathbf{H}) = 0. \tag{6}$$

The **H**-formulation considers both the air and the superconducting domain, which limits its efficiency in the calculation [30, 31]. It is used conventionally to calculate the superconductivity in HTS bulks. When considering the large aspect ratio in REBCO coated conductors ($\geqslant 10^3$), we employed the **H**-formulation based homogenisation approximation [32].

In the **T**–**A** formulation, the critical current of REBCO conductors is solved by the current vector potential **T**, and can be described as:

$$\mathbf{J} = \nabla \times \mathbf{T}. \tag{7}$$

The magnetic flux density **B** in the whole domain is solved by the magnetic vector potential **A** and can be described as:

$$\mathbf{B} = \nabla \times \mathbf{A}. \tag{8}$$

In addition, the Coulomb gauge has been used for the vector potential. The whole solution domain should satisfy the Maxwell–Ampere's circuital law as:

$$\nabla \times \nabla \times \mathbf{A} = \mu_0 \mu_r \mathbf{J}. \tag{9}$$

The transport current in REBCO coated conductors is applied to the terminals and can be described by the integral of the current density as:

$$I = \iint_S \mathbf{J} \mathrm{d}S = \iint_S \nabla \times \mathbf{T} \mathrm{d}S = \oint_{\partial S} \mathbf{T} \mathrm{d}S. \tag{10}$$

The soul of the **T**–**A** formulation is that it uses thin-strip approximation to solve the meshing issue in the model derived from the high aspect ratio of REBCO coated conductors [33, 34]; this is efficient in analysing the current transmission behaviour of specific REBCO cables with a certain number of strips. In fact, the **H**-formulation and the **T**–**A** formulation are both quite effective in calculating the electromagnetic behaviour of a certain number of REBCO coated conductors. However, when it comes to large-scale REBCO magnets that contain a large number of REBCO cables, we have to consider the **A**–**V** formulation, which is determined as follows.

The Maxwell–Faraday's equation (5) for the electrical field **E** can be expressed as:

$$\mathbf{E} = -\frac{\partial \mathbf{A}}{\partial t} - \nabla \varphi. \tag{11}$$

Here, $\nabla\varphi$ is the gradient of electrostatic potential, and we can replace it with the electrostatic contribution **V**, which is defined as a constant to maintain the current in the REBCO conductor. Consequently, equation (11) can be rewritten as:

$$\mathbf{E} = -\frac{\partial \mathbf{A}}{\partial t} - \mathbf{V}. \tag{12}$$

Combining the **E**–**J** power law in equations (1) and (12) we can derive:

$$J = J_c(B_\parallel, B_\perp, T) \sqrt[n]{-\frac{\partial A}{\partial t E_0}}. \tag{13}$$

The problem in equation (13) is that it is not smooth while $\partial A/\partial t$ equals zero. Considering the n value is an odd number. Equation (13) can be converted into the hyperbolic tangent function, which has no such defect, and which was proposed by Campbell [35] as:

$$J = J_c(B_\parallel, B_\perp, T) \tanh\left(-\frac{\partial A}{\partial t E_0}\right). \tag{14}$$

However, the collinearity between the current density and the electric field should be ensured by the proportionality rule as:

$$\partial A_x : \partial A_y : \partial A_z = J_x : J_y : J_z. \tag{15}$$

Meanwhile, the limitation on the superconducting state is defined by the current density as:

$$\sqrt{J_x^2 + J_y^2 + J_z^2} \leq J_c(B_\parallel, B_\perp, T). \tag{16}$$

Table 1. Descriptions and values of parameters in the model.

Parameter	Description	Value
E_0	Electric field constant in equations (1)–(17)	1×10^{-4} V m^{-1}
n	n-value in equations (1)–(13)	29
B_0	Flux density constant in equation (3)	0.042 65 T
u_0	The magnetic permeability of free space in equations (6) and (9)	$4\pi \times 10^{-7}$ H m^{-1}
u_r	The relative magnetic permeability in equations (6) and (9)	1
k	Constant in equation (3)	0.295 15
J_{c0}	Critical current density of the REBCO coated conductor at 77 K, self-field in equation (3)	2.8×10^{10} A m^{-2}
α	Index in equation (3)	0.5
T_c	Critical temperature of REBCO coated conductors	92 K

Therefore, the current density of a REBCO conductor that is used in the 3D computation of the toroidal field coils can be defined by combining equations (14)–(16) as:

$$\mathbf{J} = \frac{J_c(B_{\parallel}, B_{\perp}, T)}{|E|}\left[\begin{array}{c}|E_x|\tanh\left(\frac{E_x}{E_0}\right)\mathbf{i} + |E_y|\tanh\left(\frac{E_y}{E_0}\right)\mathbf{j} \\ + |E_z|\tanh\left(\frac{E_z}{E_0}\right)\mathbf{k}\end{array}\right]. \tag{17}$$

The Maxwell stress tensor has been employed to evaluate the mechanical behaviour of the toroidal field coils and is defined as:

$$\mathbf{n}T_2 = -\frac{1}{2}\mathbf{n}(\mathbf{E}\cdot\mathbf{D}) + (\mathbf{n}\cdot\mathbf{E})\mathbf{D}^{\mathrm{T}} \tag{18}$$

$$\mathbf{n}T_2 = -\frac{1}{2}\mathbf{n}(\mathbf{H}\cdot\mathbf{B}) + (\mathbf{n}\cdot\mathbf{H})\mathbf{B}^{\mathrm{T}} \tag{19}$$

where **E** is the electric field, **D** is the electric displacement, **B** represents the magnetic flux density, **H** stands for the magnetic field. T_2 is the stress tensor and can be described by a matrix. We define **n** here as the downward surface normal from the object.

The studies were carried out in the commercial finite element modelling package COMSOL Multiphysics. The physical parameters of the REBCO coated conductor refer to the experimental data at Theva Dünnschichttechnik GmbH. Specific parameters described above are presented in table 1.

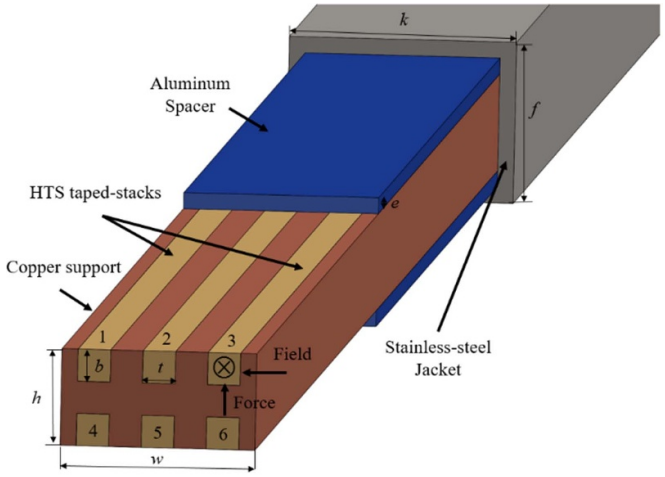

Figure 1. Diagram of the non-twisted cable.

3. System design

3.1. Cable design

The inspiration for the cable comes from combining the advantages of the viper-shaped cable and the star cable [14, 20]. It is assumed that the cable should avoid conductor torsion to protect the fragile mechanical behaviour of REBCO ceramic layers in coated conductors [39] when they are assembled into toroidal field coils. In addition, it is suggested that the number of stacked tapes mounted on the copper former should be more to reduce the proportion of copper, so that eddy-current loss induced in the copper former can be decreased. Considering the toroidal field coils are transported with DC current, the inductance induced in the cable can be ignored. Nevertheless, Joule heat generated in the non-twisted cable during charging will be studied further in the coming section. The diagram of the non-twisted cable is presented in figure 1, and geometric parameters of the cable are shown in table 2.

The cable has six stacks of tapes mounted on the copper former, with each stack containing 40 REBCO coated conductors of 4 mm in width, leading to a higher current-carrying capacity compared to the star cable. The 4 mm coated conductor was used instead of the 12 mm coated conductor to allow a reduction of the screening current along the surface of the conductor during current charging. Meanwhile, the straight-forward rectangular cable configuration can avoid the problem of uneven stress distribution. In addition, the cooling channel system has been moved out and arranged on the outside of the entire magnet system to avoid the possibility of damage by excessive stress on the cooling channels due to the large Lorentz force acting on the cable. As a result, our cable design has a few potential advantages, such as a high current-carrying capacity, great flexibility and reliability, while it is also robust and cost-effective.

3.2. Toroidal field system design

The maximum magnetic flux density produced by the toroidal field winding pack aims to reach 20 Tesla by employing the

Table 2. Descriptions of the geometric parameters of the non-twisted cable and the toroidal field winding pack.

Parameter	Description	Value
b	Height of the copper support slot	4.2 mm
e	Thickness of the aluminium spacer	2.0 mm
f	Height of the stainless-steel jacket	20.0 mm
h	Height of the copper support	12.0 mm
k	Width of the stainless-steel jacket	28.0 mm
t	Width of the copper support slot	4.2 mm
w	Width of the copper support	24.0 mm
v	Width of the REBCO stacked-tape	4.0 mm
l	Thickness of the REBCO coated conductor	0.1 mm
ri	Inner radius of the inboard leg cross-section	1000 mm
ro	Outer radius of the inboard leg cross-section	1900 mm
nu	Number of REBCO coated conductors in each taped stack	40
nc	Number of cables in a winding pack	560

non-twisted cable. The layout of the cabling system in the winding pack has been established to meet the design target and the configuration of the magnet system is shown in figure 2. Considering the high cryogenic stability of REBCO coated conductors, an indirectly cooling system is established and the non-twisted cables are cooled by thermal conduction. The helium cooling channel is on the outside of the magnet for the concern that the enormous mechanical stress generated under ultra-high fields should have small effect on the cooling system. The cooling system design has some similarities with the magnet system for the helical fusion reactor in [16]. The geometric parameters of the toroidal field winding pack are presented in table 2. The total number of non-twisted cables in a toroidal field coil is 560, and each cable contains 240 stacked-tape REBCO coated conductors.

4. Power loss and eddy-current loss of the non-twisted cable during the transient current charging procedure

The critical current of the REBCO coated conductor has been identified as being 112 A in a liquid nitrogen environment with a self-field in Theva. The value determines that the critical current density of the conductor at 77 K can reach 2.8×10^{10} A m^{-2}, which has been adopted for modelling the non-twisted cable by considering the temperature dependence.

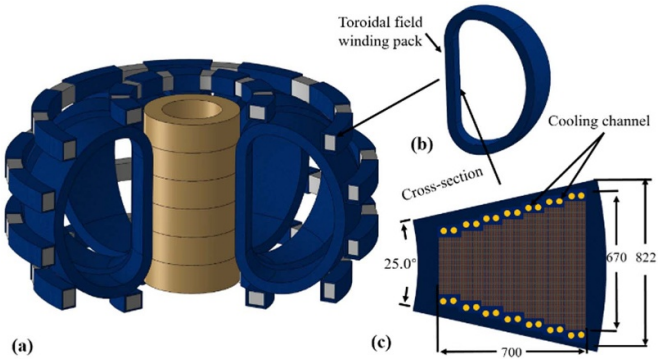

Figure 2. Diagram of the REBCO compact fusion reactor system. (a) The compact fusion reactor. (b) The toroidal field winding pack. (c) Layout of the toroidal field winding pack's inboard leg cross-section in the equatorial plane.

During the modelling procedure, a current ramping rate of 40 A s^{-1} was defined, and the charging time of the cable determined as 6 s while maintaining a current margin of more than 20%. Justification for the high ramping rate is to study the threshold power loss and dynamic magnetic flux characteristics during cable transient charging. The purpose of this section is to compare the power loss in the REBCO coated conductors and eddy-current loss in the copper support and other materials to ensure that power loss is the main loss in the cable during the transient current charging procedure, which may demonstrate that the cable design is reasonable. In addition, one concern with the non-twisted cable is that the power loss and eddy-current loss in the cable might influence the magnetic behaviour of the cable during the transient charging procedure; these effects are studied further using the **H**-formulation based finite element method.

AC current periodically reverses direction with time while DC current flows only in one direction. In the AC current transmission condition, power dissipation in REBCO coated conductors is conventionally evaluated by AC loss. However, it was discovered that the power loss in REBCO conductors is relatively small when DC current is transmitted in the conductor. The amount of power loss in REBCO stacks during the transient charging is within 10 J m^{-1} s^{-1} that is equivalent to 10 W m^{-1}, as shown in figure 3. However, the cooling power of 1 m superfluid helium cooling channel can reach 1.2×10^4 W m^{-1} [40]; which is three orders of magnitude higher than the required cooling power by the non-twisted cable.

The eddy-current loss in the copper former, the aluminium spacer and the stainless-steel jacket is also studied, as shown in figure 4. The total eddy-current loss is approximately equivalent to the power loss in one REBCO stack that is in the edge area of the conductor. It means that the main loss generated in the conductor during the transient charging procedure will still be the power loss in REBCO coated conductors. Eddy-current loss in other materials is probably 1/6 of the power loss in REBCO coated conductors. However, the loss value is small and controllable under the DC current transmission condition. It also demonstrates, however, that the Joule heat associated

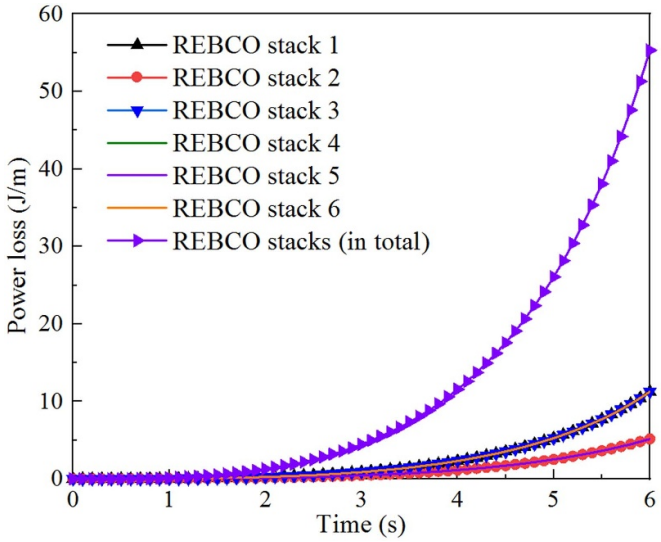

Figure 3. Power loss of the REBCO stacks in the cable during current charging at 4.2 K.

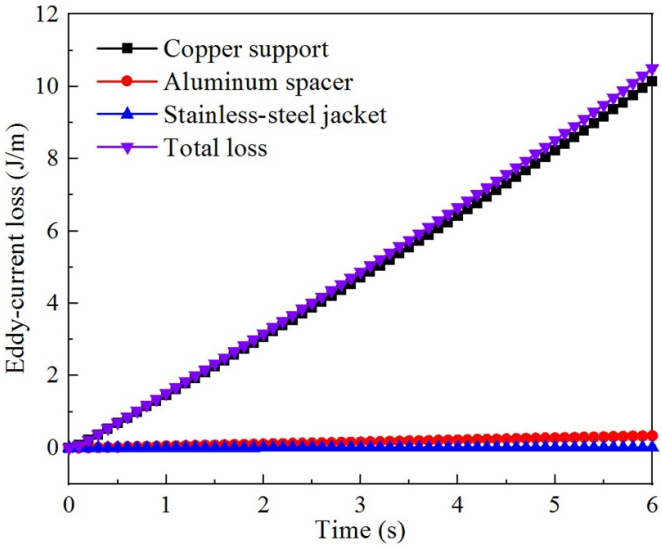

Figure 4. Eddy-current loss in the copper support, the aluminium spacer and the stainless-steel jacket during current charging in the conductor.

with power loss and eddy-current loss generated in the cable is very small under the DC current charging condition. This can be removed rapidly by ensuring the heat-exchange capacity of liquid helium in the cooling channel so as to avoid quench in superconductors.

5. Magnetic behaviour and temperature dependence of the non-twisted cable

The magnetic behaviour of the non-twisted cable is regarded as an essential factor and should be analysed before systematically studying the electromechanical behaviour of the toroidal field coils assembled from non-twisted cables. This section thus studies the magnetic behaviour of the non-twisted cable during the transient current charging procedure at 4.2 K and the maximum magnetic flux density produced by the cable under different operational temperature environments using **T–A** formulation and **H-**formulation based finite element methods. The **T–A** formulation, which is based on the thin-strip approximation, treats each REBCO coated conductor as a line strip. Therefore, the **T–A** formulation model can be considered an insulating stacked-tape coil model. However, the **H-**formulation treats the stacked-tape conductor as an equivalent anisotropic superconducting bulk. Hence, the **H-**formulation model can be regarded as a non-insulating stacked-tape coil model. It can be seen from figures 5 and 6 that the magnetic flux density calculated using the **H-**formulation seems to be slightly higher than the magnetic flux density calculated with the **T–A** formulation. A comparison of the two shows the superiority of the non-insulating coils to achieve higher fields due to current sharing between conductors. However, the differences between the two methods are relatively small. This can thus be considered negligible in the large-scale computation in the coming section.

If the cable is charging with a current ramping rate of 40 A s^{-1} at 4.2 K, a magnetic field distribution along the length of the conductor can be detected, as shown in figure 5. The field distribution initially appears to be an anomaly, but it eventually shows up as a regular wave-like shape over time. This should be an effect of the counter electromotive force resulting from the transient effect, which is calculated from Maxwell's equations considering a nonlinear current density that is, in turn, a function of the magnetic field. It indicates that the nonlinear **E–J** behaviour of superconductivity can lead to a field distortion in the initial stage of charging. However, a steady-state, wave-like magnetic field distribution along the cable at the end of charging indicates that the negative effect of the strong nonlinear **E–J** relationship on the magnetic field disappears. As a consequence, the charging for non-twisted cables can be successful. The phenomenon detected in this article has some similar inferences with the analytical solution in [29]. It demonstrates the feasibility of using non-twisted REBCO cables for the toroidal field coils of magnetic-confinement plasma devices.

The dependence of the maximum magnetic flux density of the cable on the operational temperature environment has been evaluated, as shown in figure 6. In order to achieve an ideal toroidal field for ultra-high-field magnetic-confinement devices, it is suggested that the operational temperature for toroidal field coils should not exceed 30 K. This can be achieved by a supercritical helium flow environment. Therefore, the electromechanical behaviour of toroidal field coils at 4.2 K and 30 K has been specifically studied in the coming section.

6. Electromechanical behaviour of the independent toroidal field coil

The critical current of the REBCO coated conductor is estimated to be 303.75 A at 4.2 K, 20 Tesla by referencing experimental data in [41]. It is rated to be 260 A at 30 K,

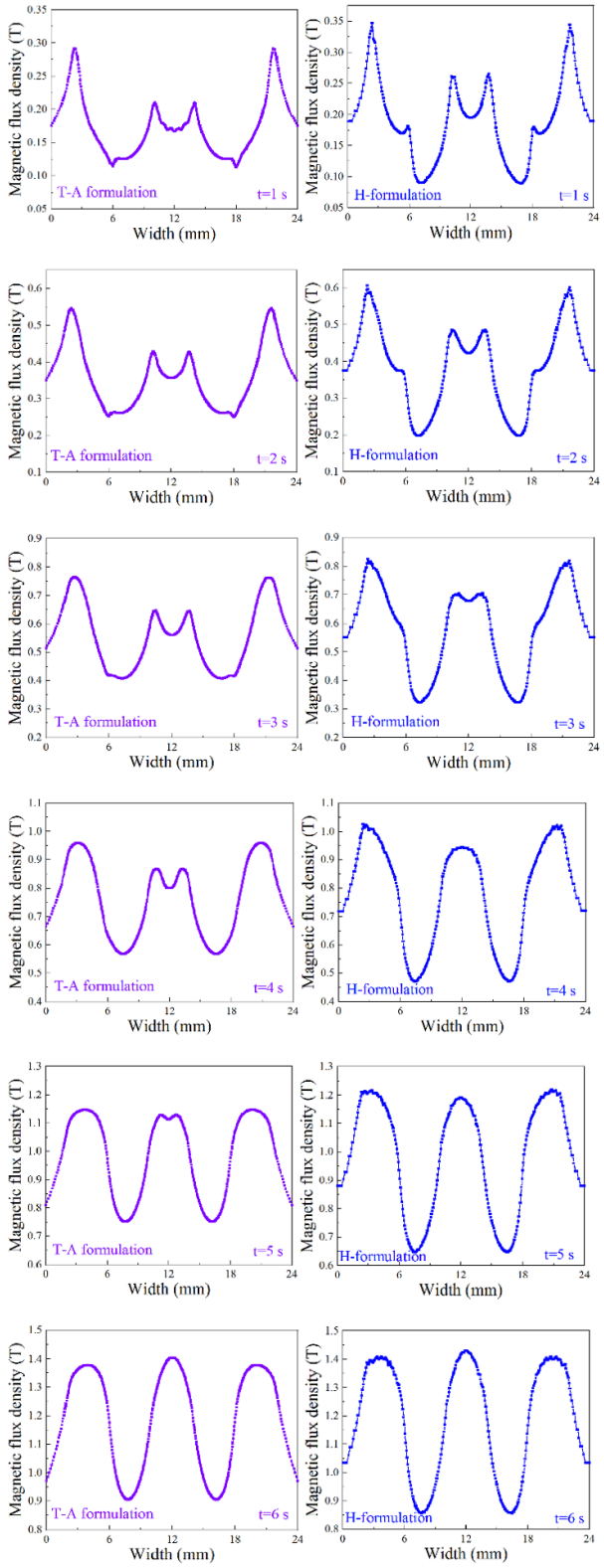

Figure 5. Wave-like magnetic fields detected from the magnet charging of the non-twisted cable by using the **H**-formulation and **T**–**A** formulation based finite element methods at 4.2 K.

20 Tesla using the Kim model. Therefore, the operating current of the REBCO coated conductor in the toroidal field coil is estimated to be 208 A at 30 K, 20 Tesla and 243 A at

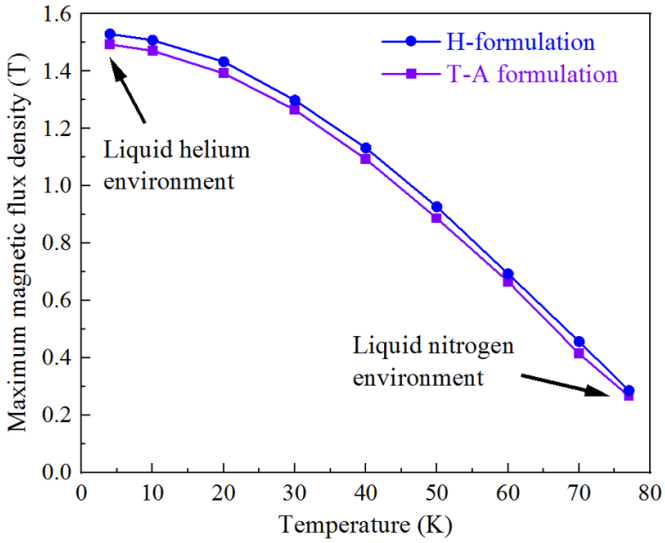

Figure 6. The dependence of the maximum magnetic flux density produced by the non-twisted cable on the temperature.

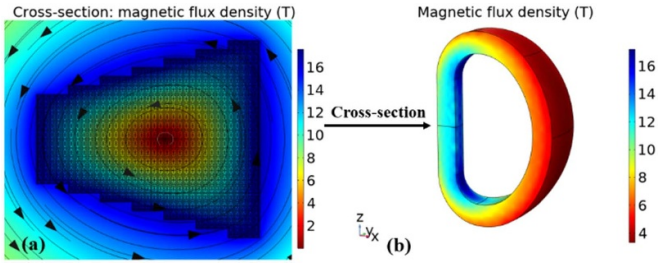

Figure 7. The magnitude of magnetic flux density produced by the independent toroidal field coil at 30 K calculated by **A**–**V** formulation. (a) Magnetic flux distribution in the cross-section of the winding pack. (b) Magnetic flux distribution of the toroidal field coil.

4.2 K, 20 Tesla, with a 20% margin to the critical current. The magnetic behaviour of the independent toroidal field winding pack has been evaluated using the **A**–**V** formulation. It could be demonstrated that the toroidal field coil assembled from non-twisted cables can achieve a maximum magnetic flux density of 17.61 Tesla at 30 K, as shown in figure 7. However, the field can exceed 20 Tesla when the operating temperature drops to 4.2 K, as shown in figure 8. The maximum magnetic flux density occurs on the edge of the toroidal field leg, which could lead to stress concentration, something that needs a specific analysis in the coming section. In addition, it can be seen from the cross-section area that cables arranged in the surroundings of the toroidal field coil could be subjected to a higher external magnetic flux density and will need to withstand more stress. If the same currents are transmitted in each conductor of the toroidal field system, cables on the edge area are more likely to be quenched.

In addition, the magnetic flux density generated by the REBCO coated conductor-based toroidal field coils may be even higher due to the magnetic superposition principle, but the critical current density of REBCO coated conductors may also fall with an increase in the external magnetic field.

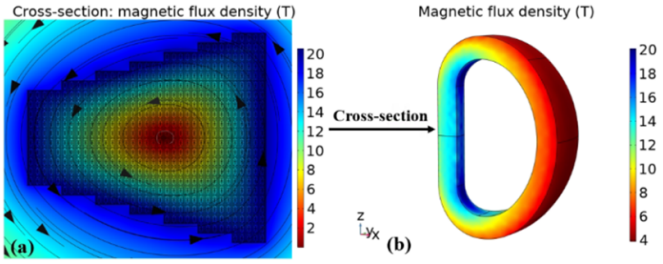

Figure 8. The magnitude of magnetic flux density produced by the toroidal field coil at 4.2 K calculated by **A**–**V** formulation. (a) Magnetic flux distribution in the cross-section of the winding pack. (b) Magnetic flux distribution of the toroidal field coil.

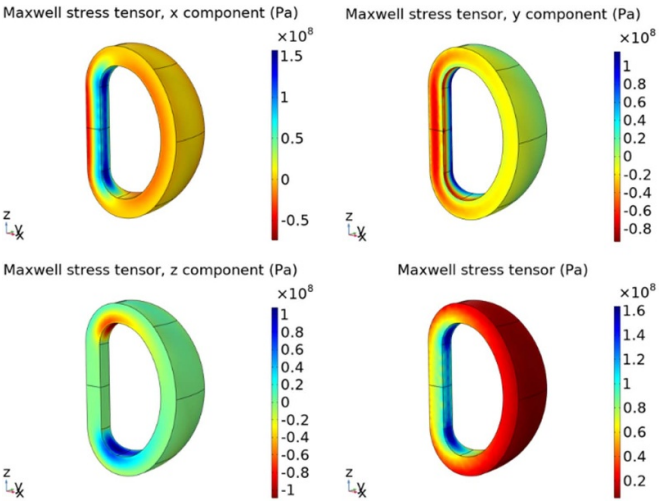

Figure 9. The distribution of Maxwell stress tensor of the toroidal field coil at 4.2 K.

However, the ultra-high critical magnetic field of the REBCO conductor determines that an ultra-high field of more than 20 Tesla for toroidal field coil modules can be achieved, and that a high field path towards large-scale fusion is possible.

The electromagnetic forces on parallel, current-carrying cables can be evaluated on the basis of the Maxwell stress tensor. The stress tolerance of CICC coated conductors is 680 MPa, and it is recommended that the stress distribution along the toroidal field coil should be less than 500 MPa [10]. The Maxwell stress tensor of the toroidal field coil and its component on the coordinate system, at 4.2 K and 30 K respectively, have been evaluated and presented in figures 9 and 10 to better determine the stress concentration in toroidal field coils. The direction of the surface normal is defined as downward as mentioned in section 2, meaning that Maxwell stresses which are in the same direction of the surface normal will be positive values. Otherwise, the values can be negative. It can be seen from the figures that the Maxwell stress of the toroidal field coil is concentrated on the inboard leg. But the maximum Maxwell stress on the toroidal field coil is within the stress tolerance of the REBCO coated conductors.

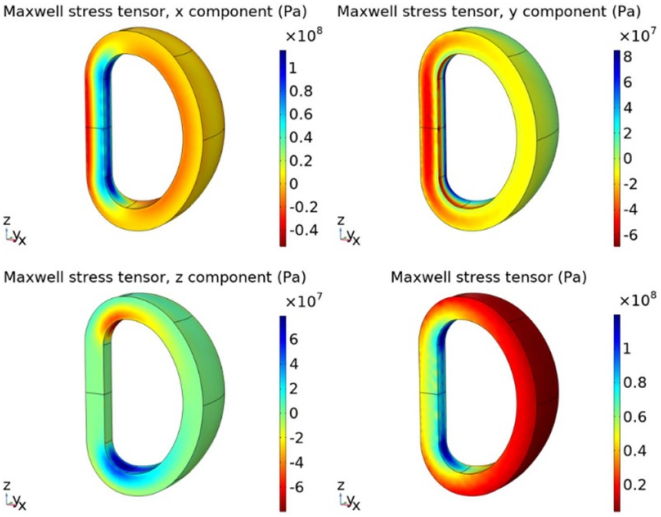

Figure 10. The distribution of the Maxwell stress tensor of the toroidal field coil at 30 K.

7. Electromechanical behaviour of the toroidal field coil modules

The Maxwell stress tensor along the toroidal field coil would be higher if all of the toroidal field coil modules are considered. Nevertheless, the critical current density of the coil modules will be mainly determined by temperature and external fields. In the same operational temperature environment, the critical current of the REBCO coated conductor can be defined by the interpolation method, with a consideration of the external magnetic fields. The concern focuses on the increasing magnetic flux density caused by the magnetic superposition principle possibly leading to a critical current degradation. Consequently, the operating current in each REBCO coated conductor of the toroidal field coil modules is defined as 148 A at 30 K and 186 A at 4.2 K, with a safety margin of more than 20% to the critical current of the REBCO coated conductor in the independent toroidal field coil. The magnetic flux distribution of the toroidal field coil modules is presented in figure 11. The upper line, middle line, and down line, which are distributed along the inner leg of the toroidal field coils in the figure have been selected as the stress concentration sites to evaluate the Maxwell stress tensor of the coil modules. In addition, a comparison of the magnetic flux density along the inner-loop of the toroidal field coil modules at 4.2 K and 30 K is presented in figure 12. The measurement starting point 0 m has been marked in figure 11, and the measurement direction is clockwise, which means that the 8 m point is in the centre of the inboard leg of the toroidal field coil.

It should be emphasised that the toroidal field coil modules are more likely to achieve a magnetic flux density of more than 20 Tesla with a relatively small transported current if an independent toroidal field coil can reach the threshold. In addition, it has been demonstrated in experiments that the independent toroidal field coil for the SPARC compact fusion reactor has achieved 20 Tesla if REBCO coated conductors are used [42].

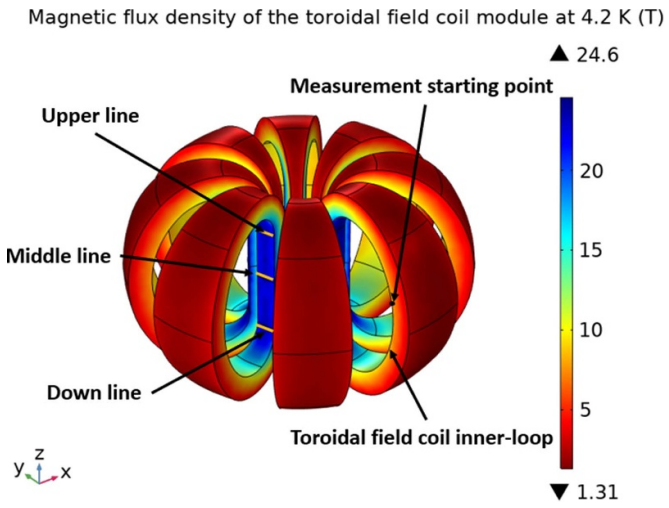

Figure 11. Distribution of the magnitude of the magnetic flux density in the toroidal field coil modules at 4.2 K.

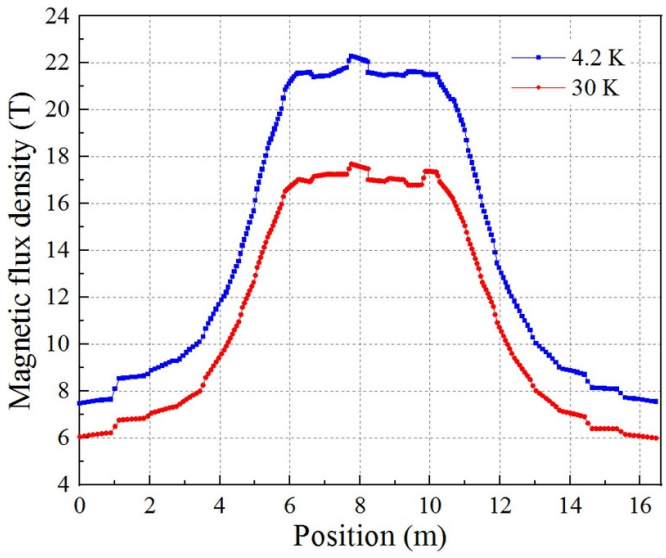

Figure 12. The magnitude of the magnetic flux density along the toroidal field coil inner-loop at 4.2 K and 30 K.

This also demonstrates the feasibility of using REBCO coated conductors to achieve ultra-high fields for large-scale fusion reactors.

The Maxwell stress distribution along the upper line, middle-line, and downline of the inboard leg of toroidal field coils is shown in figure 13. These lines have been marked in figure 11. The measurement starts from the left side of the inboard leg, the 0 mm position as shown in figure 13, and continues to the right side, the 800 mm position. The 400 mm position where the stress concentration occurs, is in the centre of the line. It can be seen from this figure that the maximum Maxwell stress is concentrated on the upper line of the inboard leg, due to the smaller bending radius. The maximum stress value is 245 MPa, within the stress tolerance of REBCO coated conductors.

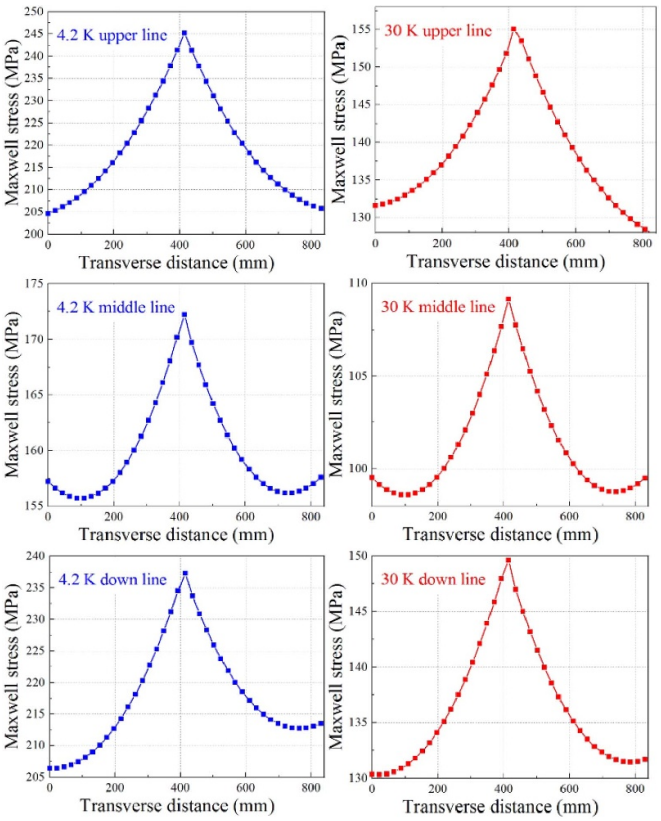

Figure 13. The distribution of Maxwell stress along the line of the toroidal field coil in the module under 4.2 K and 30 K.

8. Conclusion

A high-field path towards large-scale fusion on earth would be a landmark for fusion energy with the assistance of REBCO coated conductors that have a highly critical current density under ultra-high fields. In order to achieve the target, this paper proposed a non-twisted REBCO cable with outstanding DC current-carrying capacity. A layout for the toroidal field coils with the ability to achieve an ultra-high field of more than 20 Tesla has been designed based on this. In order to evaluate the electromagnetic behaviour of the cable, Joule heating, which is associated with power loss and eddy-current loss, and the magnetic behaviour of the cable during transient charging, have been studied further using optimised **T**–**A** formulation and **H**-formulation based finite element methods, taking temperature into consideration. It could be demonstrated that the designed non-twisted cable is able to carry ultra-high DC currents so as to achieve a high magnetic field with an operational temperature environment of between 4.2 K and 30 K. In addition, the electromechanical behaviour of the independent toroidal field coil and the toroidal field module coils have been studied further using an **A**–**V** formulation-based finite element method. It was found that the independent toroidal field coil and the toroidal field module coils are able to generate a magnetic flux density of more than 20 Tesla within the stress tolerance of REBCO coated conductors on the premise that the coils do not quench.

The study is of great significance in demonstrating the feasibility of using non-twisted REBCO coated conductor cables as a component for toroidal field coils in ultra-high-field magnetic-confinement devices. It may provide effective references for designing new-generation compact and large-scale fusion reactors by using the second-generation high temperature superconducting REBCO coated conductors.

Data availability statement

The data supporting the findings in this article is available upon reasonable request from the corresponding author.

Acknowledgments

The authors would like to thank Professor Cardella and Professor Bruzzone for their valuable suggestions on the cable design and would also like to thank the Leibniz-Rechenzentrum der Bayerischen Akademie der Wissenschaften for the use of their computational resources. In addition, the authors are very grateful to the anonymous reviewers for their comments on the manuscript, which are of great help in improving the quality of our work.

Conflict of interest

The authors have no conflicts to declare.

ORCID iDs

Xiaodong Li https://orcid.org/0000-0002-1917-6861
Dongbin Song https://orcid.org/0000-0002-5660-5610
Wenjiang Yang https://orcid.org/0000-0001-9604-112X

References

[1] Ongena J, Koch R, Wolf R and Zohm H 2016 Magnetic-confinement fusion *Nat. Phys.* **12** 398–410
[2] Mitchell N, Breschi M and Tronza V 2020 The use of Nb_3Sn in fusion: lessons learned from the ITER production including options for management of performance degradation *Supercond. Sci. Technol.* **33** 054007
[3] Strickland N M 2021 Qualifying high-temperature superconductors for fusion reactors *Supercond. Sci. Technol.* **34** 110502
[4] Iwakuma M, Tomioka A, Konno M, Hase Y, Satou T, Iijima Y, Saitoh T, Yamada Y, Izumi T and Shiohara Y 2007 Development of a 15 kW motor with a fixed YBCO superconducting field winding *IEEE Trans. Appl. Supercond.* **17** 898480
[5] Dong Y *et al* 2020 10 kV AC test verification of the high temperature superconducting fault current limiter with bias magnetic field *Cryogenics* **112** 103195
[6] Gupta R, Anerella M, Joshi P, Higgins J, Lalitha S, Sampson W, Schmalzle J and Wanderer P 2016 Design, construction, and testing of a large-aperture high-field HTS SMES coil *IEEE Trans. Appl. Supercond.* **26** 5700208
[7] Glasson N *et al* 2016 Test results and conclusions from a 1 MVA superconducting transformer featuring 2G HTS Roebel cable *IEEE Trans. Appl. Supercond.* **27** 5500205
[8] Bergen A *et al* 2019 Design and in-field testing of the world's first ReBCO rotor for a 3.6 MW wind generator *Supercond. Sci. Technol.* **32** 125006
[9] Parkinson B J, Bouloukakis K and Slade R A 2017 A compact 3 T all HTS cryogen-free MRI system *Supercond. Sci. Technol.* **30** 125009
[10] Bruzzone P, Fietz W H, Minervini J V, Novikov M, Yanagi N, Zhai Y and Zheng J 2018 High temperature superconductors for fusion magnets *Nucl. Fusion* **58** 103001
[11] Zani L *et al* 2016 Overview of progress on the EU DEMO reactor magnet system design *IEEE Trans. Appl. Supercond.* **26** 4204505
[12] Zheng J, Song Y, Liu X, Lu K and Qin J 2018 Overview of the design status of the superconducting magnet system of the CFETR *IEEE Trans. Appl. Supercond.* **28** 4204305
[13] Zheng J, Kang R and Song Y 2016 Electromagnetic and stability study on HTS/LTS hybrid superconducting central solenoid *IEEE Trans. Appl. Supercond.* **26** 4205505
[14] Yanagi N, Goto T, Miyazawa J, Tamura H, Terazaki Y, Ito S, Tanaka T, Hashizume H and Sagara A 2019 Progress in the conceptual design of the helical fusion reactor FFHR-d1 *J. Fusion Energy* **38** 147–61
[15] Sagara A, Tamura H, Tanaka T, Yanagi N, Miyazawa J, Goto T, Sakamoto R, Yagi J, Watanabe T and Takayama S 2014 Helical reactor design FFHR-d1 and c1 for steady-state DEMO *Fusion Eng. Des.* **89** 2114–20
[16] Yanagi N, Ito S, Terazaki Y, Seino Y, Hamaguchi S, Tamura H, Miyazawa J, Mito T, Hashizume H and Sagara A 2015 Design and development of high-temperature superconducting magnet system with joint-winding for the helical fusion reactor *Nucl. Fusion* **55** 053021
[17] Novikov M S, Ivanov D P, Novikov S I and Shuvaev S A 2015 Current-carrying element based on second-generation high-temperature superconductor for the magnet system of a fusion neutron source *Phys. At. Nucl.* **78** 1148–54
[18] Creely A J *et al* 2020 Overview of the SPARC tokamak *J. Plasma Phys.* **86** 865860502
[19] Celentano G, de Marzi G, Fabbri F, Muzzi L, Tomassetti G, Anemona A, Chiarelli S, Seri M, Bragagni A and Della Corte A 2014 Design of an industrially feasible twisted-stack HTS cable-in-conduit conductor for fusion application *IEEE Trans. Appl. Supercond.* **24** 4601805
[20] Hartwig Z S *et al* 2020 VIPER: an industrially scalable high-current high-temperature superconductor cable *Supercond. Sci. Technol.* **33** 11LT01
[21] Mulder T, Dudarev A, Mentink M, Silva H, van der Laan D, Dhalle M and ten Kate H 2016 Design and manufacturing of a 45 kA at 10 T REBCO-CORC cable-in-conduit conductor for large-scale magnets *IEEE Trans. Appl. Supercond.* **26** 4803605
[22] Uglietti D, Bykovsky N, Sedlak K, Stepanov B, Wesche R and Bruzzone P 2015 Test of 60 kA coated conductor cable prototypes for fusion magnets *Supercond. Sci. Technol.* **28** 124005
[23] Terazaki Y *et al* 2017 Current-carrying capability of the 100 kA-class HTS STARS conductor for the helical fusion reactor FFHR-d1 *J. Phys.: Conf. Ser.* **871** 012099
[24] Li X, Song D, Wu Y, Liu Y, Yang W and Macian-Juan R 2022 Current-carrying capability and magnetic behavior of the HTS twisted stacked-tape conductor cable for the compact fusion reactor *IEEE Trans. Appl. Supercond.* **32** 4200205
[25] de Marzi G, Allen N C, Chiesa L, Celentano G, Takayasu M, Tomassetti G, Augieri A and Della Corte A 2016 Bending tests of HTS cable-in-conduit conductors for high-field magnet applications *IEEE Trans. Appl. Supercond.* **26** 4801607
[26] de Marzi G, Celentano G, Augieri A, Marchetti M and Vannozzi A 2021 Experimental and numerical studies on

current distribution in stacks of HTS tapes for cable-in-conduit-conductors *Supercond. Sci. Technol.* **34** 035016
[27] Mulder T, Weiss J, van der Laan D, Dudarev A and Kate H T 2020 Recent progress in the development of CORC cable-in-conduit conductors *IEEE Trans. Appl. Supercond.* **30** 4800605
[28] Uglietti D, Kang R, Wesche R and Grilli F 2020 Non-twisted stacks of coated conductors for magnets: analysis of inductance and AC losses *Cryogenics* **110** 103118
[29] Lelekhov S A 2021 Analysis of a possibility to use parallel non-twisted stacks of HTS tapes as cable in high current conductor of tokamak toroidal field coils *IEEE Trans. Appl. Supercond.* **31** 1–5
[30] Shen B, Francesco G and Tim C 2020 Overview of H-formulation: a versatile tool for modeling electromagnetics in high-temperature superconductor applications *IEEE Access* **8** 2996177
[31] Berrospe-Juarez E, Trillaud F, Zermeño V M R and Grilli F 2021 Advanced electromagnetic modeling of large-scale high-temperature superconductor systems based on H and TA formulations *Supercond. Sci. Technol.* **34** 044002
[32] Zermeno V M R, Abrahamsen A B, Mijatovic N, Jensen B B and Sørensen M P 2013 Calculation of alternating current losses in stacks and coils made of second generation high temperature superconducting tapes for large scale applications *J. Appl. Phys.* **114** 173901
[33] Zhang H, Zhang M and Yuan W 2016 An efficient 3D finite element method model based on the T–A formulation for superconducting coated conductors *Supercond. Sci. Technol.* **30** 024005
[34] Huber F, Song W, Zhang M and Grilli F 2022 The TA formulation: an efficient approach to model the macroscopic electromagnetic behaviour of HTS coated conductor applications *Supercond. Sci. Technol.* **35** 043003
[35] Campbell A M 2007 A new method of determining the critical state in superconductors *Supercond. Sci. Technol.* **20** 292
[36] Ruiz-Alonso D, Coombs T and Campbell A M 2004 Computer modelling of high-temperature superconductors using an A–V formulation *Supercond. Sci. Technol.* **17** S305
[37] Brandt E H 1996 Superconductors of finite thickness in a perpendicular magnetic field: strips and slabs *Phys. Rev.* B **54** 4246
[38] Patel A and Glowacki B A 2012 Enhanced trapped field achieved in a superconducting bulk using high thermal conductivity structures following simulated pulsed field magnetization *Supercond. Sci. Technol.* **25** 125015
[39] Plakida N 2010 *High-Temperature Cuprate Superconductors: Experiment, Theory, and Applications* vol 166 (Berlin: Springer Science & Business Media)
[40] Lebrun P and Tavian L 2015 Cooling with superfluid helium *CERN Yellow Rep.* **15** 07156
[41] Tsuchiya K *et al* 2017 Critical current measurement of commercial REBCO conductors at 4.2 K *Cryogenics* **85** 1–7
[42] Zach H *et al* 2021 The SPARC toroidal field model coil *MT-27 Conf.*